Axial transport within bidisperse granular media in horizontal rotating cylinders

J. R. Third,[1,*] D. M. Scott,[2] and C. R. Müller[1]

[1]*Institute of Energy Technology, Department of Mechanical and Process Engineering, ETH Zürich, Leonhardstrasse 27, CH-8092 Zürich, Switzerland*

[2]*Department of Chemical Engineering and Biotechnology, University of Cambridge, Pembroke Street, Cambridge CB2 3RA, United Kingdom*

(Received 21 January 2011; revised manuscript received 7 June 2011; published 7 October 2011)

The discrete element method has been used to examine axial dispersion within rotating cylinders containing two sizes of particle. Two bed configurations are considered: initially segregated, which consists of a pulse (narrow axial band) of small particles within a bed of large particles, and initially mixed, in which the cylinder is loaded with a homogeneous mixture of the two particle sizes. The dispersion of the small particles within initially segregated beds is found to depend strongly on the initial length of the pulse of small particles. Initially mixed beds are found to undergo a transient period in which the small particles disperse rapidly. Following this transient, axial dispersion of both particles sizes is found to follow Fick's second law, in that the mean squared deviation of the axial position of the particles is proportional to time. Axial dispersion coefficients have been calculated for initially mixed beds that have reached steady state; the axial dispersion coefficients of both particle sizes decrease as the volume fraction of small particles is increased.

DOI: 10.1103/PhysRevE.84.041301 PACS number(s): 45.70.Mg, 83.10.Rs, 83.80.Fg

I. INTRODUCTION

One of the most intriguing properties of granular materials is their tendency to segregate by size or density when agitated. An experiment that is often used to demonstrate segregation is the partially filled, horizontal rotating cylinder. When a rotating cylinder is loaded with a mixture of materials that differ in size or density, two types of segregation can occur: (i) radial segregation, in which the smaller or denser particles form a central core in the bed cross section, and (ii) axial segregation, which leads to the formation of bands with different compositions along the rotational axis of the cylinder. Radial segregation is a fast process and is usually completed within a few cylinder rotations, whereas axial segregation is a much slower process and does not always occur.

In the development of models of axial segregation it is often assumed that segregation is opposed by a dispersive flux that obeys Fick's law [1]. However, despite the importance of the axial dispersion coefficient in these models, relatively little is known about axial dispersion within bidisperse systems and the axial dispersion coefficient is often assumed to be a constant or to depend only on the particle type. Those studies that have considered axial transport within bidisperse systems have been restricted to cases in which the two grain types are initially segregated. Compared to initially mixed systems, these systems have the advantage that the initial condition is well defined, which allows the particle motion to be quantified more easily in experiments. However, it is unclear whether findings from studies based on initially segregated systems are applicable to the initially mixed case that is the usual initial condition for axial segregation experiments.

Nakagawa *et al*. [2] studied the axial migration of binary mixtures created using different sizes of oil-filled pharmaceutical spheres. Two types of initial condition were employed: a two-band initial condition and a three-band, or pulse, initial condition. The two-band initial condition was created by dividing the cylinder in two in the axial direction and loading the two ends of the cylinder with different particle types. The pulse initial condition consisted of a pulse or narrow axial band of small particles located axially in the center of the cylinder with large particles on either side. Nakagawa *et al*. [2] reported that the rate of axial migration increased with the size ratio between the particles and noted that, when the two-band initial condition was used, axial mixing was asymmetric because the small particles were able to penetrate the area initially occupied by large particles more easily than the large particles could penetrate the region initially occupied by small particles.

Ristow and Nakagawa [3] used magnetic resonance imaging (MRI) to study the dispersion of 1- and 4-mm spheres in a two-band configuration. Dispersion was found to be influenced by radial segregation; the small particles moved into the region initially occupied by large particles as a core in the center of the bed's cross section while the large particles moved into the region initially occupied by the small particles on the surface of the bed. Based on these observations, Ristow and Nakagawa [3] argued that dispersion within their system may be concentration dependent since the composition of the bed at any axial position will control the environment experienced by the particles.

Dury and Ristow [4] used the discrete element method (DEM) to simulate beds consisting of two particle sizes arranged in a two-band initial condition. Axial dispersion of the small particles was found to follow Fick's second law such that the mean square deviation in particle position increases linearly with time, as shown by Eq. (1):

$$\frac{1}{N'}\sum_{k=1}^{N'}[z_k(t)-z_k(0)]^2 = 2D_{\mathrm{ax}}t. \tag{1}$$

Here D_{ax} is the dispersion coefficient, z is the axial particle position, and N' is the number of particles whose position is being considered. The dispersion coefficient for the small particles was found to depend on the rotation speed of the drum and the coefficient of friction and particle density of the

*jthird@ethz.ch

small particles, having a minimum when the densities of the two particle types were equal.

Khan and Morris [5] used an optical projection technique to study the evolution of a pulse of small particles within a bed of larger, translucent particles. The volume fraction of small particles at a particular axial position was assumed to be proportional to the square of the height of the core of small particles measured by the projection technique. Based on these measurements, dispersion of the small particles was found to be subdiffusive such that the mean square deviation in particle position would be expected to increase as t^{β} with $0 < \beta < 1$. However, Fischer *et al.* [6] compared the results of the projection techniques used by Khan and Morris [5] with MRI measurements and found the projection technique to give a poor representation of the concentration of small particles.

Taberlet and Richard [7] performed DEM simulations of a pulse of 5-mm spheres within a bed consisting of 10-mm spheres. Dispersion of the pulse of 5-mm particles was found to follow Fick's second law.

Fischer *et al.* [6] used MRI to investigate the dispersion of a pulse of small spheres within a bed of larger spheres, and of a pulse of large spheres within a bed of small spheres. The dispersion of the pulse of small spheres into the bed of large spheres was found to be Fickian. However, the dispersion of the pulse of large spheres was found to be subdiffusive, which Fischer *et al.* [6] attributed to a concentration-dependent diffusion coefficient.

In this work we examine the axial motion of particles within initially segregated and initially mixed bidisperse systems using the DEM.

II. SIMULATION METHOD

The soft-sphere DEM, which is used in this work, is well documented in the literature [8] and is not described here except to detail the particular force laws used in this work. In the normal direction a damped linear spring is employed and attractive forces between particles are prevented such that the force in the normal direction, F_n, for a collision between particles i and j is given by

$$F_n = \max(0, k_{n_{ij}}\delta_n - 2\eta_n\sqrt{m_{ij}k_n}v_n). \tag{2}$$

Here η_n is the damping factor in the normal direction, δ_n is the particle overlap, k_n is the normal stiffness, v_n is the relative velocity in the normal direction, and m_{ij} is the effective mass defined as $1/m_{ij} = 1/m_i + 1/m_j$. In the tangential direction static friction is modeled as a damped linear spring and the magnitude of the tangential force is limited by Coulomb's law such that

$$F_t = \min(\mu k_{n_{ij}}\delta_n, k_{t_{ij}}\delta_t - 2\eta_t\sqrt{m_{ij}k_t}v_t). \tag{3}$$

Here μ is the coefficient of friction, η_t is the damping factor in the tangential direction, k_t is the tangential stiffness, and v_t is the relative velocity of the two surfaces in contact. The tangential displacement, δ_t, is defined as $\int v_t dt$. Table I shows the parameter values of the system, which is taken to be the base case in this work. A particle size distribution given by

$$p(d) = \frac{d_{\min}d_{\max}}{d_{\max} - d_{\min}}\frac{1}{d^2}, \quad d_{\min} < d < d_{\max}, \tag{4}$$

TABLE I. Base case simulation parameter values.

Name	Symbol	Value
Nominal diameter of small particles	d_s	1.0 mm
Nominal diameter of large particles	d_l	2.2 mm
Particle size distribution		±5%
Particle density	ρ	1000 kg/m^3
Normal spring stiffness	k_n	1000 N/m
Tangential spring stiffness	k_t	500 N/m
Normal damping factor	η_n	0.22
Tangential damping factor	η_t	0.2
Particle coefficient of friction	μ_p	0.5
Acceleration due to gravity	g	9.81 m/s^2
Diameter of cylinder	D	48 mm
Length of cylinder	L	240 mm
Rotation speed of cylinder	Ω	30 rpm
Time step for numerical scheme	dt	1.6×10^{-6} s

is used for both particle sizes in all simulations [9]. The bounds on this distribution, $d_{\min}$ and $d_{\max}$, are 95% and 105% of the nominal particle size.

The cylinder in which the particles are rotated is modeled as a smooth, but frictional, cylinder onto which "wall rougheners" have been attached. The wall rougheners serve to prevent slip between the cylinder wall and the outermost particles in the bed. They consist of lines of 1-mm particles running along the length of the cylinder and are placed 5 particle diameters apart, center to center, around the cylinder circumference. The centers of the wall rougheners are on the cylinder circumference. More details concerning the use of wall rougheners to prevent slip within rotating cylinders modeled using the DEM are given by Third *et al.* [10]. The ends of the cylinder are modeled as flat, frictionless end plates. Other than the friction coefficient of the end caps, the physical properties of the cylinder and the end caps are identical to those of the particles. The equations of motion are integrated using a third-order Adams-Bashforth scheme with a time step, dt, which satisfies $dt \leqslant t_{\text{col}}/30$, where t_{col} is the minimum duration of a binary collision.

In this work both initially mixed and initially segregated systems are considered. The initially mixed states are generated by arranging particles on a regular rectangular lattice. The size of each particle within the lattice is chosen based on the value of a random number to give the desired ratio of small and large particles. The particles are assigned a random velocity and are allowed to fall into the bottom of the cylinder under gravity. Once the particles come to rest, the cylinder rotation is started. Time, t, is defined as zero at this point. The volumetric fill level of the initially mixed beds studied in this work is approximately 48%. For the initially segregated states the cylinder is loaded with particles using dividers to separate the regions of small and large particles. After the rotation has started, the cylinder is allowed to rotate for 2 s (one rotation of the cylinder) to ensure that the bed has reached steady state at its dynamic angle of repose. Finally the dividers are removed while the cylinder is rotating. For this system, time is defined to be zero when the dividers are removed.

The initially segregated systems considered here consist of a pulse of 1-mm particles in the center of a bed of 2.2-mm particles; see Fig. 1. The length of the pulse of small particles,

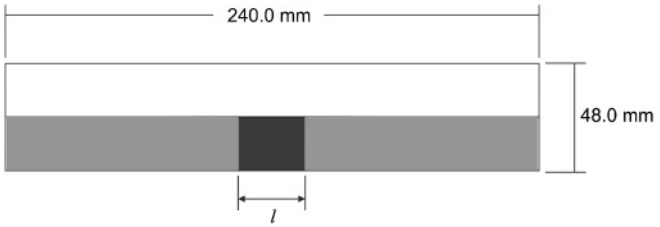

FIG. 1. Schematic showing the configuration of initially segregated systems. The darker shading represents small particles and the lighter shading represents large particles.

l, is either 6 or 30 mm and the fill levels of both 1- and 2.2-mm particles are approximately 43%.

III. RESULTS

Figure 2 shows the mean square deviation in the axial position of a pulse of 1-mm particles versus time for two different values of l. For both pulse lengths the data shown have been averaged over six simulations performed using different values for the random seed. Averaging the data in this way helps to reduce the noise on the data for larger values of t. The mean square deviations for homogeneous beds of both 2.2- and 1-mm particles are also shown. The parameters for these homogeneous simulations are identical to those used when two types of particles are present except that, for the 1-mm particles, a cylinder length of 120 mm was used in order to reduce the computational load. For these homogeneous systems the mean square deviation was calculated based on a pulse of particles located axially in the center of the cylinder. Further details regarding the calculation of the mean square deviation for homogeneous systems were given by Third *et al*. [11].

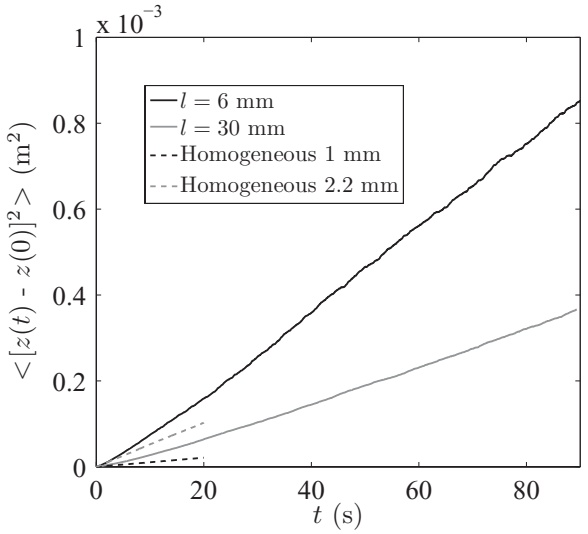

FIG. 2. Mean square deviation in axial position vs time. The continuous lines show the deviations for the 1-mm particles for two pulse lengths of 1-mm particles within a bed of 2.2-mm particles. The dashed lines show the deviations for homogeneous beds. The cylinder has a diameter of 48 mm, a length of 240 mm, and is rotated at 30 rpm. The fill level of both particle sizes is approximately 43%.

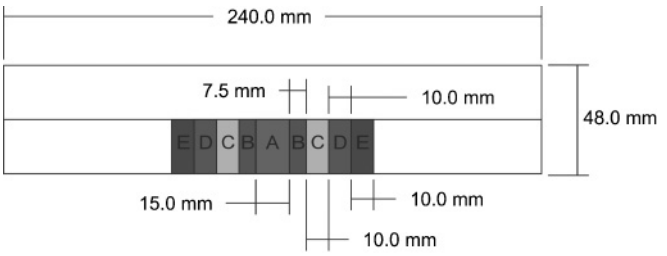

FIG. 3. Schematic showing the initial location of the axial slices considered in Fig. 4.

The data shown in Fig. 2 demonstrate that the dispersion of the small particles in this initially segregated system does not follow Fick's second law for all values of t. The slope of the line representing the $l = 30$ mm case increases with time, indicating that the rate of axial dispersion increases with t. Such behavior could be described as superdiffusive; however, the authors do not recommend such a description since, as is demonstrated below, this behavior is not characteristic of the steady state of the system. For the $l = 6$ mm case the rate of axial dispersion increases for the first 25 s but reaches an approximately constant value after this time.

Figure 2 also indicates that the mean square deviation for the small particles is considerably larger for $l = 6$ mm than for $l = 30$ mm. This result suggests that small particles located near the interface with the large particles disperse faster than those located farther from the interface since the only significant difference between the two pulse lengths is the proportion of the small particles located at the interface: for $l = 6$ mm a larger fraction of the small particles are located near the interface than for $l = 30$ mm. To investigate further the effect of the interface on axial dispersion, the $l = 30$ mm case shown in Fig. 2 is divided into axial slices as shown by Fig. 3. Slices A and B contain only small particles, while slices C, D, and E contain only large particles. Figure 4 shows the mean square deviation versus time for particles which were initially located in these different axial slices. The mean square deviation for

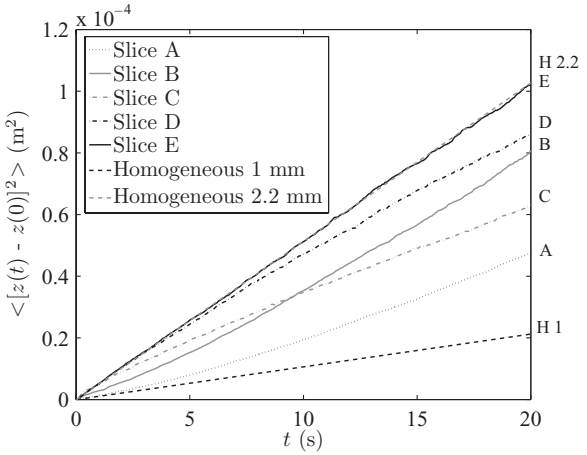

FIG. 4. Mean square deviation for particles initially located in the axial slices shown in Fig. 3. The cylinder has a diameter of 48 mm, a length of 240 mm, and is rotated at 30 rpm. The fill level is approximately 43%.

homogeneous beds of both 2.2- and 1-mm particles are again shown.

Consider first slices C, D, and E, which contain only large particles and are located progressively farther from the initial interface between the two particle types, with slice C closest to the interface and slice E farthest from it. There is good agreement between the mean square deviation of the particles initially located in slice E and that of a homogenous bed of large particles. This indicates that far from the interface the bed behaves as a homogeneous bed of large particles. For slice C the mean square deviation follows that of a homogeneous bed of large particles for approximately 1 s but for larger t the dispersion is smaller than that of the homogeneous case. It is thought that this deviation is due to the presence of small particles that reduce the dispersion of the large particles. The mean square deviation of slice D shows similar behavior to slice C in that it initially follows the dispersion expected for a homogeneous bed, but it disperses less than the homogeneous case at larger values of t. For slice D the deviation from the homogeneous case occurs later than for slice C, at about 5 s, and for later times the deviation from the homogeneous case is less pronounced. This is consistent with the deviation from homogeneous behavior being caused by interactions with small particles because particles initially located in slice D will take longer to come into contact with small particles than those in slice C and will experience a lower concentration of small particles than particles initially in slice C.

Slices A and B, which contain only small particles, show that the dispersion of small particles is also affected by the interface with the large particles. For slice B, located at the interface between the two particle sizes, the dispersion is significantly larger than that of a homogeneous bed of 1-mm particles for all times. Furthermore, the gradient of the mean square deviation increases with time. It is thought that this is due to the increase in the concentration of large particles experienced by the particles in this slice as time increases. Slice A is located at the center of the pulse of 1-mm particles and initially follows the dispersion expected for a homogeneous bed of 1-mm particles. However, at larger times the concentration of large particles experienced by slice A will increase, causing an increase in the axial dispersion of this pulse.

The results presented above suggest that the axial transport within this system is concentration dependent such that dispersion of the small particles is increased in the presence of large particles and the dispersion of the large particles is reduced in the presence of small particles. To investigate further the influence of composition on axial dispersion within bidisperse systems, simulations of systems which are initially well mixed have been performed.

In this work axial transport within initially mixed systems is quantified by calculating the mean square deviation of particles within a 150-mm slice centered on the midpoint of the cylinder. The mean square deviation in the axial position of this group of particles is calculated every 0.02 s for 20 s. After 20 s a new central slice is selected and the process is repeated. The mean square deviations calculated using this procedure have been found to be independent of the length of the central slice used in the calculation. This indicates that the axial motion of the particles within this slice is not affected by the cylinder end caps. In the following the mean square deviations of the 1- and 2.2-mm particles within the slice of particles being considered are calculated separately. Note that, although a higher concentration of small particles was observed close to the end caps, none of the systems studied here underwent axial segregation in the central region in which measurements were made. Furthermore, the number of each type of particle within this region remained approximately constant once the bed reached steady state.

Figure 5(a) shows the mean square deviation against time for the 1-mm particles within a bed containing 25% 1-mm particles by volume. The eight lines on the graph represent slices of particles selected at different times and the times shown in the legend indicate the value of t when the slice of particles was selected. These data indicate that, following an initial transient, a steady state is reached in which the mean square deviation of the small particles increases linearly with time. This suggests that, after the initial transient, dispersion

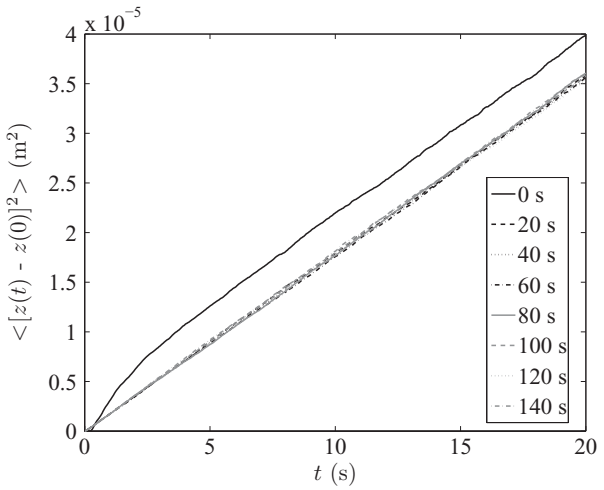

(a) Small particles

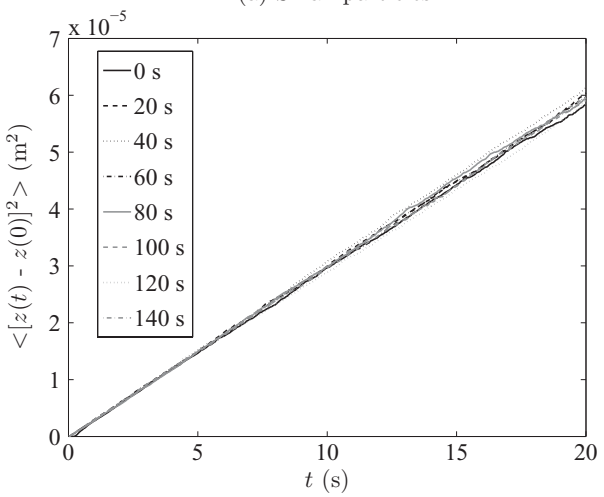

(b) Large particles

FIG. 5. Mean square deviation vs time for a bed containing 25% small particles by volume. Times given in the legend indicate the value of t at which $z(0)$ was evaluated. Mean square deviation of the (a) small and (b) large particles. The cylinder has a diameter of 48 mm, a length of 240 mm, and is rotated at 30 rpm. The fill level is approximately 48%.

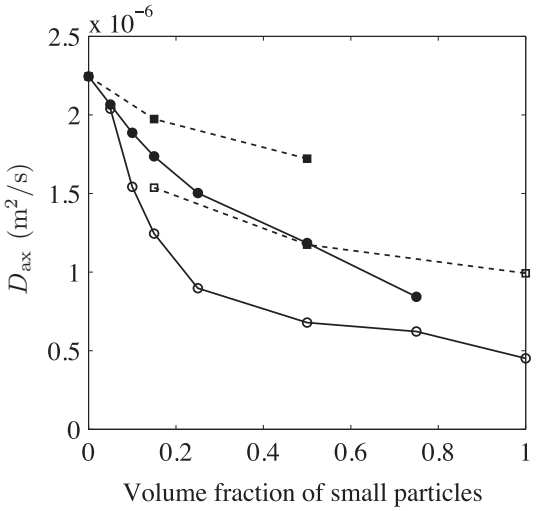

FIG. 6. Axial dispersion coefficients for initially mixed beds:○, dispersion coefficient of 1-mm particles in a bed composed of 1- and 2.2-mm spheres; •, dispersion coefficient of 2.2-mm particles in a bed composed of 1- and 2.2-mm spheres; □, dispersion coefficient of 1.5-mm particles in a bed composed of 1.5- and 2.2-mm spheres; ■, dispersion coefficient of 2.2-mm particles in a bed composed of 1.5- and 2.2-mm spheres. The cylinder has a diameter of 48 mm, a length of 240 mm, and is rotated at 30 rpm. The fill level is approximately 48%.

of the small particles obeys Fick's second law, allowing the steady-state dispersion coefficient, D_{ax}, to be calculated based on the gradient of a plot of mean square deviation against time. The mean square deviation of the 2.2-mm particles within this bed is shown in Fig. 5(b). These data indicate that the dispersion of these particles reaches its steady state shortly after the cylinder has started to rotate and that the steady-state dispersion of the large particles obeys Fick's second law. The analysis described above has been conducted for initially mixed beds with a range of volume fractions of 1-mm particles. Following an initial transient all of the systems studied were found to obey Fick's second law. Figure 6 show values of D_{ax} obtained for initially mixed beds of 1- and 2.2-mm particles as a function of the volume fraction of 1-mm particles. These data indicate that the axial dispersion coefficient of both species is concentration dependent and decreases monotonically as the volume fraction of small particles is increased.

Further simulations have been performed to analyze the influence of the particle size ratio (d_l/d_s) and the drum diameter on dispersion within initially mixed beds. Axial dispersion coefficients for initially mixed beds composed of 1.5- and 2.2-mm spheres are shown in Fig. 6. Other than the diameter of the small particles, the simulation parameters for these simulations are identical to those given in Table I. These data indicate that increasing the size of the small particles in an initially mixed bed increases the axial dispersion coefficient of both the small and large particles. This is consistent with the findings of Parker *et al.* [12] and Third *et al.* [11], who reported that the dispersion coefficient of monodisperse spheres increases as the particle size is increased.

Table II gives axial dispersion coefficients of initially mixed beds for cylinder diameters of 48 and 96 mm. A small particle diameter of $d_s = 1.5$ mm was used for these simulations and

TABLE II. Axial dispersion coefficients for initially mixed beds composed of 1.5- and 2.2-mm spheres. Data shown for drum diameters of 48 and 96 mm and beds composed of 15% and 50% small particles by volume. The cylinder has a length of 240 mm and is rotated at 30 rpm. The fill level is approximately 48%.

	D_{ax} (m²/s)			
	15%		50%	
D (mm)	1.5 mm	2.2 mm	1.5 mm	2.2 mm
48	1.54×10^{-6}	1.97×10^{-6}	1.17×10^{-6}	1.72×10^{-6}
96	1.73×10^{-6}	1.95×10^{-6}	1.18×10^{-6}	1.73×10^{-6}

all other simulation parameters were identical to the base case values given in Table I. For beds composed of 50% small particles by volume the axial dispersion coefficients of both particle sizes are independent of the cylinder diameter. Dispersion of the 2.2-mm particles in beds composed of 15% small particles by volume is also independent of the cylinder diameter. These results are consistent with results for beds composed of monodisperse particles [11,12], which have indicated that, for sufficiently large D, the cylinder diameter has no influence on axial dispersion. However, Table II indicates that, for beds composed of 15% small particles by volume, dispersion of the 1.5-mm particles does not follow this trend. The dependence of the dispersion coefficient of these particles on the cylinder diameter is not currently understood and warrants further investigation.

IV. DISCUSION

Taberlet and Richard [7] used the DEM to examine the dispersion of a 125-mm pulse of 5-mm particles into a bed of 10-mm particles. Dispersion of this pulse was found to follow Fick's second law. This result appears to be in agreement with the data shown in Fig. 2 which indicate that, following an initial transient, the mean square deviation increases linearly with time for both values of l. Taberlet and Richard [7] also studied axial dispersion within beds consisting of only 5-mm spheres and only 10-mm spheres. Axial dispersion was found to be Fickian for both sizes of particles. D_{ax} was found to have the same value for beds containing only 5-mm particles, only 10-mm particles, and for the pulse of 5-mm particles within a bed of 10-mm particles. While the data in Fig. 2 suggest that it should be possible to select a value of l such that the dispersion of the pulse is similar to that of a bed of large particles, it is surprising that D_{ax} was found to be independent of d_p for beds containing only one particle type. Both the experiments of Parker *et al.* [12] and the DEM calculations of Third *et al.* [11] found that axial dispersion within beds consisting of a single particle type depends strongly on the particle diameter. The reasons for these discrepancies are currently not understood, although it is noted that the force laws used by Third *et al.* [11] differed from those employed by Taberlet and Richard [7].

Fischer *et al.* [6] used MRI to investigate the dispersion of a pulse of 2-mm spheres in a bed of 4-mm spheres and of a pulse of 4-mm spheres in a bed of 1.5-mm spheres. Axial dispersion of the small spheres was found to follow Fick's second law but dispersion of the large spheres was found to be subdiffusive.

This subdiffusive behavior was attributed to a concentration-dependent diffusion coefficient. Fischer *et al*. [6] reported that D_{ax} for the large particles within their system increased as the concentration of large particles increased but were unable to extract the exact concentration dependence of D_{ax}. It is surprising that concentration dependence was observed for the large particles but not for the small particles because any mechanism that affects the dispersion of one species would also be expected to influence the dispersion of the other species. In this work D_{ax} for 1- and 2.2-mm particles has been calculated for initially mixed systems that have been allowed to reach steady state. The data presented in Fig. 6 for the 2.2-mm particles are consistent with the observation made by Fischer *et al*. [6] that the dispersion of the large particles increases as their concentration increases. Unlike Fischer *et al*. [6] this study has found that the dispersion of the smaller, 1-mm particles is also concentration dependent. It is likely that the discrepancy between these results arises from the different methods used in the two studies. Fischer *et al*. [6] studied the dispersion of a pulse of particles and considered concentration dependence as a mechanism by which the dispersion of this pulse may deviate from Fickian dispersion. The results for $l = 6$ mm in Fig. 2 show that, following an initial transient, the mean square deviation in particle position for a pulse of small particles may increase linearly with time, indicating Fickian dispersion and, based on the criterion employed by Fischer *et al*. [6], no concentration dependence. However, when the data for the two pulse widths are compared it is clear that the dispersion of these particles is concentration dependent.

A possible explanation for the concentration dependence reported above may be obtained by considering the displacement of a particle that moves past a stationary "obstacle" particle in a densely packed system. Figure 7 shows a schematic of two such particles in the case that the particles are of equal size. In order for the particle to pass the obstacle it must undergo a displacement in the plane perpendicular to its velocity. Axial dispersion will occur when this displacement has a component parallel to the axis of the cylinder. The magnitude of the displacement required to pass the obstacle in this way may, on average, be expected to depend on the sum of the radii of the particles involved in the collision. Consequently, the displacement of a small particle passing a large obstacle particle will be larger than that of a small particle passing a small obstacle, and the displacement of a large particle passing a small obstacle will be smaller than that of a large particle passing a large obstacle. This is consistent with the observations made above that the presence of small particles decreases the dispersion of the large particles while dispersion of the small particles is enhanced in the presence of larger particles.

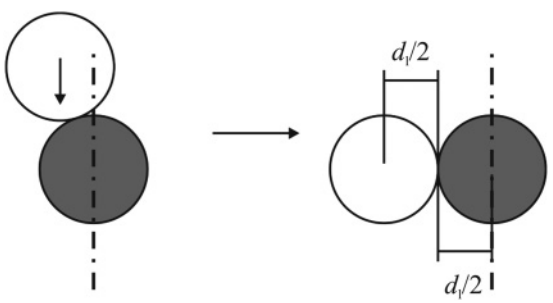

FIG. 7. Schematic of a particle (unshaded) moving past an obstacle of equal size (shaded).

The initially mixed systems considered here are found to undergo a transient period followed by Fickian dispersion. This initial transient may be due to the onset of flow within the cylinder, radial segregation, or a combination of the two. The behavior of these systems is consistent with the model proposed by Third *et al*. [11], who argued that axial dispersion within a horizontal rotating cylinder should be expected to obey Fick's second law if the system is at steady state, if the bed is homogeneous in the axial direction, and if the particles are periodically stationary in the axial direction. An initially mixed system that does not undergo axial segregation is expected to satisfy these criteria once radial segregation is complete.

V. CONCLUSIONS

Axial transport within beds composed of two types of particles has been investigated using the DEM. Two bed configurations have been considered: initially segregated, which consists of a pulse of 1-mm particles located axially in the center of a bed of 2.2-mm particles, and initially mixed, in which the bed is loaded with a homogeneous mixture of small and large particles. Both bed configurations evolve with time: the pulse of small particles in the initially segregated bed spreads out into the area occupied by large particles, whereas the initially mixed system undergoes radial segregation. These changes in bed configuration cause the rate of axial dispersion to change with time and lead to behavior that might be termed subdiffusive or superdiffusive. For the systems studied here this behavior is not representative of the steady-state behavior of the system.

For the initially segregated systems considered here the dispersion of the small particles was found to be influenced strongly by the initial length of the pulse of small particles. This indicates that the interaction between the two particle sizes plays an important role in axial dispersion within these beds.

The initially mixed beds were found to undergo an initial transient during which the mean square deviation of the small particles increases rapidly. Once the bed reaches steady state the axial dispersion of both particle sizes is found to follow Fick's second law such that the mean square deviation in axial position increases linearly with time. Axial dispersion coefficients have been calculated for initially mixed beds that have reached steady state. These data indicate that the dispersion coefficient for both particle sizes decreases as the volume fraction of 1-mm particles is increased.

ACKNOWLEDGMENTS

The authors would like to thank Stuart Scott for his contribution in developing the DEM code and in modeling and Peter Benie and Tilman Koschnick for their advice and assistance. J.R.T. would like to thank the Engineering and Physical Sciences Research Council (EPSRC) for financial support.

[1] K. M. Hill and J. Kakalios, Phys. Rev. E **52**, 4393 (1995).
[2] M. Nakagawa, J. L. Moss, K. Nishimura, and T. Ozeki, in *Powders and Grains 97*, edited by B. Behringer and J. Jenkins (Balkema, Rotterdam, 1997), pp. 447–450.
[3] G. H. Ristow and M. Nakagawa, Phys. Rev. E **59**, 2044 (1999).
[4] C. M. Dury and G. H. Ristow, Granular Matter **1**, 151 (1999).
[5] Z. S. Khan and S. W. Morris, Phys. Rev. Lett. **94**, 048002 (2005).
[6] D. Fischer, T. Finger, F. Angenstein, and R. Stannarius, Phys. Rev. E **80**, 061302 (2009).
[7] N. Taberlet and P. Richard, Phys. Rev. E **73**, 041301 (2006).
[8] P. A. Cundall and O. D. L. Strack, Géotechnique **29**, 47 (1979).
[9] T. Pöschel and T. Schwager, *Computational Granular Dynamics: Models and Algorithms* (Springer-Verlag, Berlin, 2005).
[10] J. R. Third, D. M. Scott, S. A. Scott, and C. R. Müller, Granular Matter **12**, 587 (2010).
[11] J. R. Third, D. M. Scott, and S. A. Scott, Powder Technol. **203**, 510 (2010).
[12] D. J. Parker, A. E. Djkstra, T. W. Martin, and J. P. K. Seville, Chem. Eng. Sci. **52**, 2011 (1997).